IX International Conference on Computational Methods in Marine Engineering
MARINE 2021
I.M. Viola and F. Brennan (Eds)

# NUMERICAL MODELLING OF WATER BALLAST. APPLICATION TO FISH CAGES

**D. PRIOUR***

* Ifremer Centre Bretagne
Laboratoire Comportement des Structures en Mer
29280 Plouzané, France
e-mail: daniel.priour@ifremer.fr

**Key words:** Ballast, Numerical modelling, Fish cage, Flexible pipe

**Abstract.** To withstand harsh sea states, fish cages can be immersed during critical sea state conditions. In this paper, we present the numerical modelling of water ballast in flexible pipe. According to our results, we consider this modelling to be easy to implement, easy to use, and numerically efficient. We use the finite element method, in which the pipes are modelled using bar elements. The volume of the ballast tank is distributed over the extremities of the bar elements and is represented as cubes. Once the volume of water ballast has been determined, the altitude of the free surface of the ballast is calculated by dichotomy in the cubes. The force on the extremities of the bar elements is calculated using the resulting altitude. Comparison of the present numerical modelling with an analytical method shows that for a vertical tube, the present modelling is robust and realistic. Through the modelling we have assessed the behaviour of a fish cage using ballast: We analysed the shape of the cage during the different phases (immersed, emerged, ballasting, unballasting), the tension in mooring lines, and in the floating part of the cage.

## 1. INTRODUCTION

To withstand harsh sea states, fish cages can be immersed during harsh sea state conditions. This technique is used, or has been used, in the French overseas islands of Réunion and Guadeloupe. In these tropical zones, metocean conditions are considered reasonably acceptable for floating structures for most of the year and in harsh conditions during rare periods. Harsh conditions are generally generated by cyclones which can be accurately predicted allowing fish farmers sufficient time to immerse their cages.

On the east coast of Guadeloupe, fish farmers use the technique of cage immersion (figure 1): generally speaking, the cages are emerged (left of figure 1) when metocean conditions are calm; and on rare occasions, when metocean conditions are expected to be rough, the cages are immersed (right of figure 1). The cages used are traditional: they are made of rings of PEHD pipes, cylindrical netting and moorings and are immersed by using water as ballast. Generally speaking, ballast is any heavy material carried temporarily or permanently in a vessel to provide desired draft and stability. Here, ballast is water carried temporarily in the cage to provide desired immersion. The ballast tank here is composed of the main floats (PEHD pipes) of the cages.

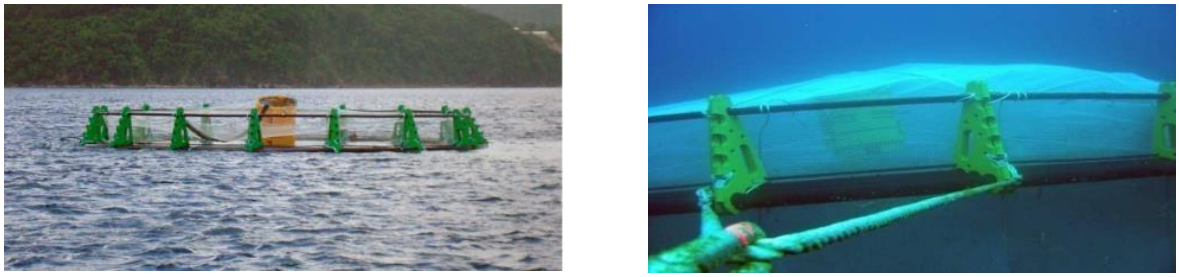

Figure 1: Fish cage. The float of the cage is composed of two concentric PEHD pipes which are also used as the ballast tank. Left: The pipes are empty of water ballast and consequently the cage is emerged. Right: The pipes are full of water ballast and the cage is immersed

The objective of the present work was to study the behaviour of such fish cages using water ballast: What are the intermediate shapes of the cage during immersion and emersion? What is the variation of cage volume during these phases? As far as we know, there is little research work available on this subject. In [1], Beveridge explains the reason for using submerged cages: the movement of water particles decreases exponentially with depth and consequently the hydrodynamic force on the cage. Kim et al [2] compare results of a numerical model with model tests and in-situ measurements. The numerical model in their work is focused on the air and water transfer in the ballast tank and the fish cage is reduced to only one numerical node. As far as we know, there is no easy-to-use numerical modelling of cage deformation due to ballast. This can also be modelled using CFD or SPH but these models induce large computational time. In this paper, we propose numerical modelling of water ballast in pipes, easy to implement, easy to use and numerically efficient.

The present study is based on previous works on the numerical modelling of flexible structures made of netting and cables, including fish cages [3].

## 2. HYPOTHESIS AND METHOD

### 2.1. Finite element method

The numerical modelling used here is founded on the finite element method (FEM). This method models the net using a triangular element ([5], [4]) and the cables, pipes, and chains are modelled using bar elements ([3], [4]). For netting and bar elements, the FEM model considers inner tension, drag force due to water speed, weight, buoyancy and drag on the bottom. The modelling of water ballast in pipes is described later in this paper.

The FEM model considers all nets and cables; so, for a fish cage, the mooring lines, buoys, PEHD rings and netting are considered.

### 2.2. The modelling of water ballast in pipes

In this chapter, we describe the modelling of forces due to the ballast.

In this modelling, ballast is possible in the pipes. As previously mentioned, theses pipes are modelled as bar elements. which means that they are straight. They have two extremities; each extremity has three Cartesian coordinates.

A ballast tank is defined by a group of pipes (two pipes in figure 2). Each pipe of the ballast tanks has a volume dedicated to the water ballast. In figure 2, these ballast tank volumes have been determined at 0.25133m³ for the right-hand pipe and 0.14137m³ for the left-hand pipe. There is also a volume of ballast inside the ballast tank which is between 0m³ and the sum of volumes dedicated to the ballast (this sum is 0.3927m³ for figure 2).

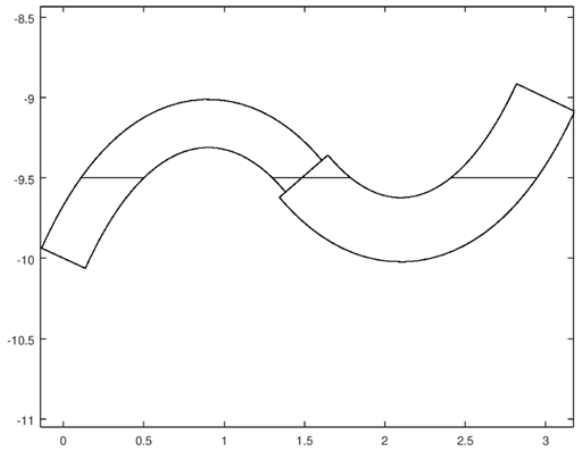


Figure 2: Side view of a ballast tank made of two pipes. The free surface of the water ballast is at -9.5m altitude.

The volume of ballast tank of each pipe is firstly equally spread between the bar elements defining the pipe. This ballast tank volume per bar is secondly equally spread over each extremity of the bar element: 0.0419m³ (0.25133/3/2) for the nodes of the pipe on the right of figure 3, and 0.0236m³ (0.14137/3/2) on the left. These ballast tank volumes are cubic and are shown in figure 3. These cubes are oriented along axes X, Y and Z. The size of the cube depends on the volume of ballast tank affected to the pipe and on the number of bar elements modelling the pipe: Figure 3 shows that the cubes of the pipe on the right are larger than on the left.

The volume of water ballast inside the ballast tank is determined by the user (0.207m³ for figure 3). This volume of ballast determines a free surface inside the ballast tank which is the same value for each cube of all pipes. In figure 3, this altitude is -9.5m. The water ballast in the ballast tank is shown as grey zones. Except for two nodes at the extremities, there are two cubes for each node as the node is the extremity of two consecutive bar elements, as shown on the middle node.

Once the volume of water ballast has been determined by the user ($0.207m^3$ for figure 3), the altitude of the free surface of the ballast is calculated by dichotomy (-9.5m for figure 3). This calculation uses a minimal and maximal altitude. The minimal is the minimal value between the altitude of each node of the ballast tank minus half the side of the cube. So, the

maximal is the maximal value between the altitude of each node of the ballast tank plus half the side of the cube.

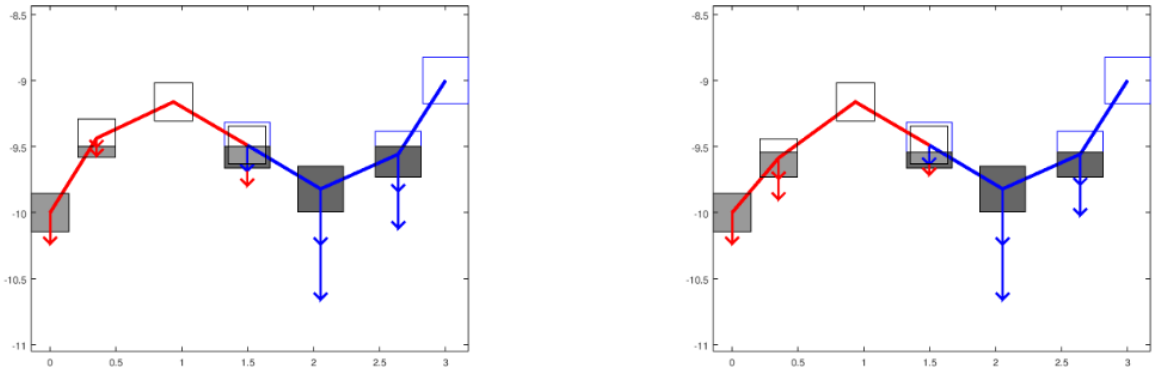


Figure 3: Both pipes in figure 2 are modelled by 3 bar elements, and the ballast tank is modelled by cubes. The grey zones represent the water ballast. The arrows represent the weight of water ballast. On the left, the model represents figure 2. On the right, the second node on the left is lower by 0.15m. This lower position leads to a larger quantity of water affected to this node. Consequently, the water affected to other nodes could be smaller (e.g. node in the middle).

To clarify this aspect of our modelling, if the position of node changes, the water ballast affected by node could consequently change: on the right of figure 3, the same structure is represented excepted that one node (second on the left) is lower. Consequently, the water ballast affected to this node increases when the quantity of other nodes may decrease (node in the middle and the second on the right). It shows that the weight of water ballast of these nodes has changed (arrows on left versus right on figure 3).

Because the numerical model uses a finite element method, it uses forces on nodes. Once the altitude is calculated, the ballast volume is calculated per cube. From this volume two forces are calculated:

- The weight of ballast per node is the water ballast volume in each cube multiplied by the density of water and by gravity. Figure 3 shows these forces as vertical arrows: Obviously, the greater the ballast, the greater the weight.

- If the ballast is dynamic, this means that the ballast varies with time. This can occur on immersing fish cages. In this case, the user has to determine a table in which the volume of the ballast is function of time. For dynamic cases we may consider, using Newton's second law, force (***F***) due to change in momentum:

$$F = \frac{\partial(M.V)}{\partial t} \tag{7}$$

Which gives

$$F = \frac{\partial M}{\partial t}V + M\frac{\partial V}{\partial t} \tag{8}$$

*M* is the mass of ballast per node (Kg), ***V*** the speed vector of node (m/s), $\frac{\partial M}{\partial t}$ is the variation of the mass of ballast per second per node (Kg/s), $\frac{\partial V}{\partial t}$ is the acceleration vector of the node ($m/s^2$).

In the following example, we use the shape of pipes as in figure 2. This example uses 33 bar elements for each pipe. The dichotomy gives an altitude of the free surface at -9.521m. The ballast tank volumes and the water ballast volume are the same as in figure 3 but the altitude is slightly different (-9.521m on figure 4 vs -9.50m on the left of figure 3), this is due to the number of bar elements which is larger in figure 4 than in figure 3.

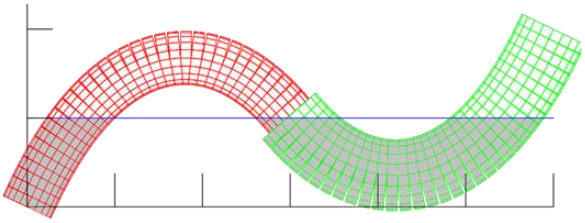

Figure 4: Calculation of two pipes of figure 2. The altitude of the ballast is shown. Each pipe is modelled with 33 bar elements.

## 3. RESULTS

### 3.1. Verification on a still vertical tube

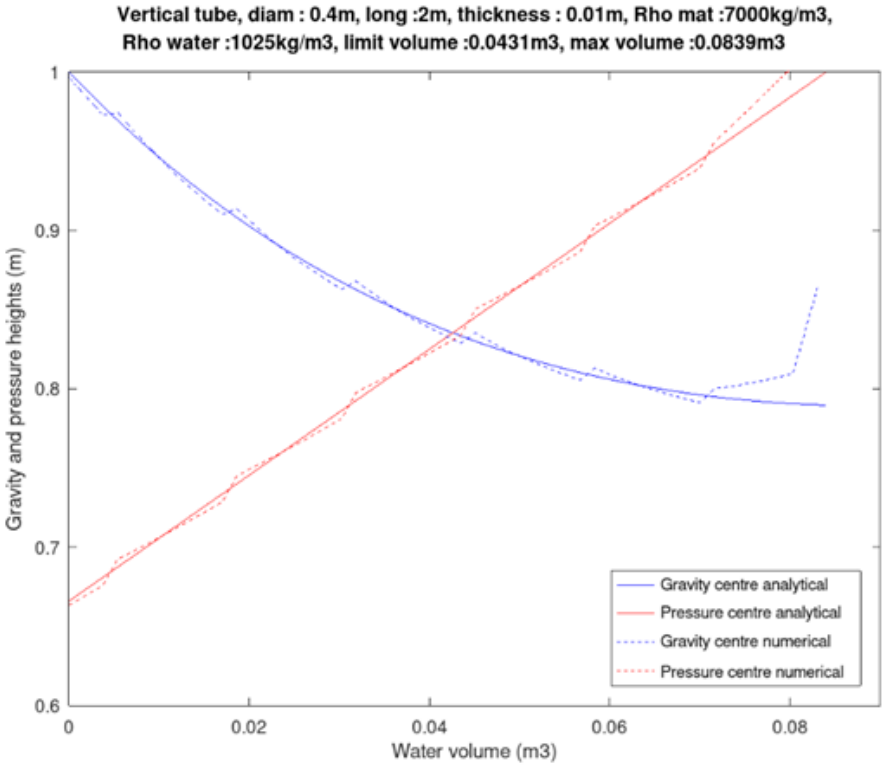

Figure 5: Position of centres of gravity and buoyancy of a vertical pipe, relative to the base of the pipe, depending on water ballast volume. Solid lines are analytical results and dotted lines are numerical (calculated with the present model). From analytical results, a ballast volume below 0.0431 m³ means that the tube is unstable vertically and the pipe sinks when ballast volume is above 0.0839 m³. The analytical and numerical curves are similar.

In this case, the tube remains vertical. It is 2 m long ($L$), 0.4 m in diameter ($\Phi$) with a thickness of 0.01 m ($ep$). This thickness is only considered for the surround of the tube: the extremities are closed without thickness. This choice of extremities without thickness, was made to simplify the analysis. The density of tube wall is 7000Kg/m³ ($\rho m$) which leads to a density of 682.5Kg/m³ for the whole tube (mass of wall divided by the tube volume). The density of water is 1025Kg/m³ ($\rho$, sea water).

The tube is stable vertically when the centre of gravity is below the centre of buoyancy. The centres of gravity ($HG$) and buoyancy ($HB$) are calculated depending on the quantity of water ballast ($WV$). In the following all the distances are relative to the base of the tube.

The global (tube alone plus water ballast) position of the gravity centre ($HG$, m) relative to the base of the tube is assessed:

$$HG = \frac{\frac{L}{2}MT + HWWV\rho}{MT + WV\rho} \tag{9}$$

The position of the buoyancy centre ($HB$) relative to the base of the tube is assessed using the total mass and the section of the tube:

$$HB = \frac{2(\frac{MT}{\rho} + WV)}{\pi\Phi^2} \tag{10}$$

*MT:* mass of the tube alone (Kg)

*HW*: centre of gravity of the water ballast (m)

In figure 5 (solid lines) the parameters $HG$ and $HB$ have been drawn in function of $WV$. It shows that the height of the gravity centre is at the middle of the tube (1m) when there is no ballast, as expected. It shows that the volume of ballast at which tube stability changes is 0.0431m³. Above 0.0431m³, the tube is stable vertically: the centre of gravity ($HG$) is below the centre of buoyancy ($HB$). Below 0.0431m³, the tube is unstable: the gravity centre is above the buoyancy centre.

When the volume of the ballast is above 0.0839m³ the tube sinks. Consequently, the weight of the tube plus the weight of the ballast is not supported by the buoyancy of the whole tube. If the tube is close to sinking it means that the whole 2 m of tube is in the water and consequently the height of the buoyancy centre is 1 m, as shown in figure 5: when the water volume is 0.0839m$^3$ the height of buoyancy is 1 m.

The stability of the vertical tube is calculated using the present numerical model. The tube is divided into 19 bar elements. Bar element density is 682.5Kg/m³ in order to represent the mass of the tube wall. The flexion rigidity of bar elements is 48950647N.m², which has been calculated using a Young modulus of 210GPa, which is a usual value for steel. The volume of the ballast tank is 0.2268 m³, which corresponds to volume of a cylinder of 2m in length and a diameter of 0.4 m minus twice a thickness of 0.01 m.

The volume of water ballast varies between 0.083 m³ to 0 m³ in 2000s.

The numerical model gives a result (dotted lines figure 5) similar to the analytical calculation (figure 5 solid lines).

Also, a “stair effect” can be seen on the dotted curves of figure 5: the two curves vary in steepness. This is due to the modelling of the ballast tank in cubes: two adjoining cubes may overlap, when cubes overlap gravity and buoyancy centres rise slower with an increase of the ballast than when the cubes do not overlap.

### 3.2. Verification on a tube initially vertical

This verification concerns the equilibrium of a tube in relation to the volume of the ballast. The tube is the one used in the previous example except that now it can bend.

The tube has an initial ballast of 0.083 m³, which is the limit before sinking. The ballast volume decreases to 0 m³ over 2000s. We also introduced a wave of a 2-second period and 0.01m high. Without the wave, the tube remains vertical, as there is no horizontal force on the tube to initiate inclination.

Figure 6 shows that the tube is almost vertical (inclination ~ pi/2) when the ballast is large, and since the ballast is close to 0.042 m³ the tube is almost horizontal (inclination ~0). The water volume of 0.042 m³ representing the point when the tube topples horizontally is similar to the value considered in the analytical study (see figure 5, 0.0431 $m^{3,}$ solid lines).

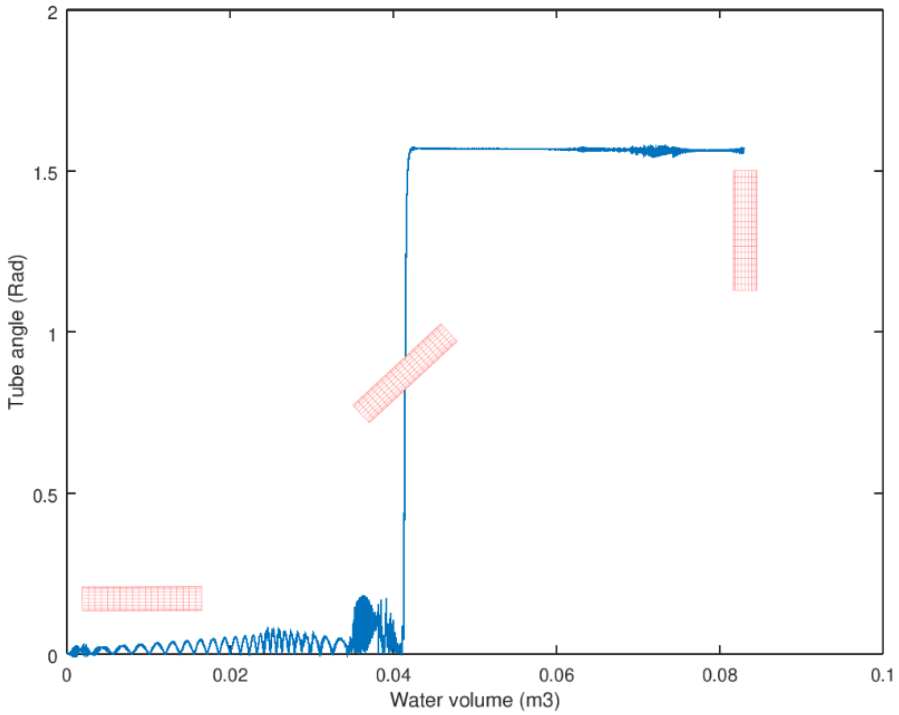


Figure 6: Inclination of tube due to water ballast calculated with the present model. The tube is vertical (tube angle ~ pi/2) when ballast is between 0.083 and 0.0414 m³. The tube is horizontal (tube angle ~0) for a ballast between 0.0414 m³ and 0 m³. The tube is at pi/4 for a ballast of 0.0414 m³.

Some cases have been calculated with a different number of bar elements in the tube. For each case, the ballast volume required to bend the tube at pi/4 is calculated and reported in Table 1. This volume remains almost constant, close to the analytical value 0.0431 m³, but always smaller. This constancy shows that this modelling is relatively robust.

| Element number | Limit volume (m³) |
|---|---|
| 1 | 0.0405 |
| 3 | 0.0430 |
| 4 | 0.0425 |
| 7 | 0.0413 |
| 11 | 0.0413 |
| 19 | 0.0414 |

Table 1: Ballast volume required for changing stability of the tube. Volumes calculated from the present model depend on the number of bar elements modelling the tube. The volumes are close to the analytical value (0.0431 m³).

### 3.3. Application to an Antilles-type fish cage

This modelling is applied to a cage used in French Antilles. The cage is moored on a site with a depth of 32 m. In this study, there is no current (figure 7).

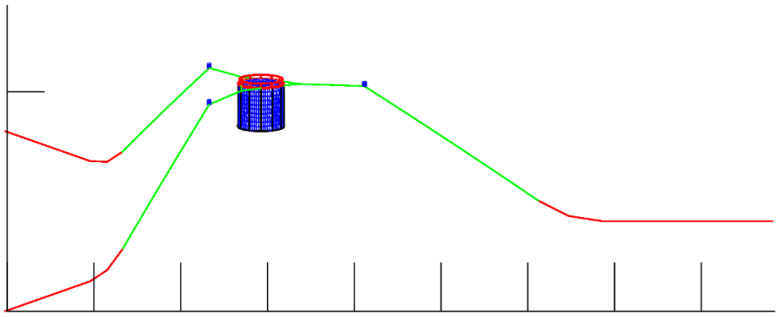

Figure 7: 3D view of the modelling of the fish cage and its mooring.

The floating part (visible on figure 7 and figure 13) is made of an internal ring (diameter 0.2 m, length 31.416 m), an external ring (diameter 0.2 m, length 33.3m), 12 spacers between the internal and external rings (diameter 0.2 m, length 0.3 m), a handrail (diameter 0.16 m, length 31.416 m) and 12 feet between the internal ring and the handrail (diameter 0.16 m, length 1 m). The thickness of all these components is 0.01 m, the Young modulus is 1E+9N/m², and the density of the material is 950Kg/m³. The following parameters can be deduced: elongation stiffness (EA, Young modulus multiplied by the material section) of components of diameter 0.2 m is 6 MN and 5 MN for diameter 0.16 m. EI is 27010N.m² for diameter 0.2 m and 13312N.m² for diameter 0.16m.

The netting has a mesh side of 0.01 m long, a diameter of 0.002 m, a density of 1100Kg/m³ and an elongation stiffness (EA) of 2000 N. The top and bottom netting panel total 386404 meshes, when the netting around the cage has 3120000 meshes: 1000 mesh bars along the height and 6240 around the cage.

The netting is pulled taut by a heavy ring (visible in figure 9, diameter 0.1 m, length 33.3m, density of 2032 Kg/m$^3$, flexion rigidity of 2898N.m$^2$). This ring is connected to the external ring by 12 ropes of 10 m in length, a diameter of 0.036 m, and a density of 950Kg/m³. The ring is linked to the netting by 12 ropes of 0.3 m in length, a diameter of 0.036 m, and a density of 950Kg/m³.

The mooring consists of three lines consisting of, from the bottom to the cage, a chain, a rope, a buoy, a surface rope, and two bridles. The characteristics of chains (ropes, buoys, surface ropes, bridles): 55 (48, 1, 15, 5) m long, 0.065 (0.036, 0.8, 0.036, 0.036) m in diameter, 3758 (850, 390, 850, 850) Kg/m$^3$ of density and 6 (1, 30, 1, 1) MN of elongation stiffness.

The bottom extremities of the chains are equally spaced on a circle of 118 m radius, these extremities are fixed to the bottom.

The floating parts carry the ballast tank. The ballast tank volume per floating part is 0.804m$^3$ for the internal ring, 0.852 m$^3$ for the external ring, 0.096$^3$ for the spacers, 0.180 m$^3$ for the feet and 0.480m$^3$ for the handrail. That means a maximal ballast volume of 2.412 m$^3$.

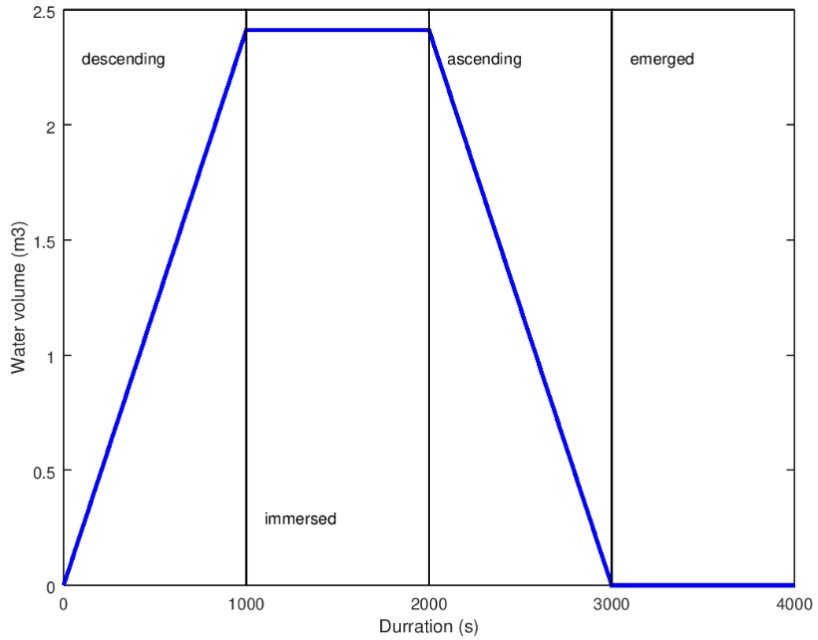


Figure 8: Variation of ballast. This variation depends on time and is determined by the user. The maximal volume is 2.412 m³ (table 3) when the minimal is 0 m³. The movement and position of the cage are noted: descending, immersed, ascending and emerged.

The ballast varies as shown in figure 8 and is determined by the user:

- From 0 m³ to volume available in the ballast tank (2.412 m³) during the first 1000s, the cage descends,
- It remains at the maximum for the following 1000s, the cage is then totally immersed,
- It decreases to 0 m³ over the next 1000s, the cage ascends,
- It remains at 0 m³ for the last 1000s, the cage has emerged.

Some shapes of the cage are shown in figure 9. The volume inside the cage is calculated and shown in figure 10. Thus, most of the time the volume remains close to the maximal volume (800 m³). The minimal value is 717 m³ and occurs during unballasting when the ballast is at 80% of the ballast tank and when the cage is ascending (figure 9 d).

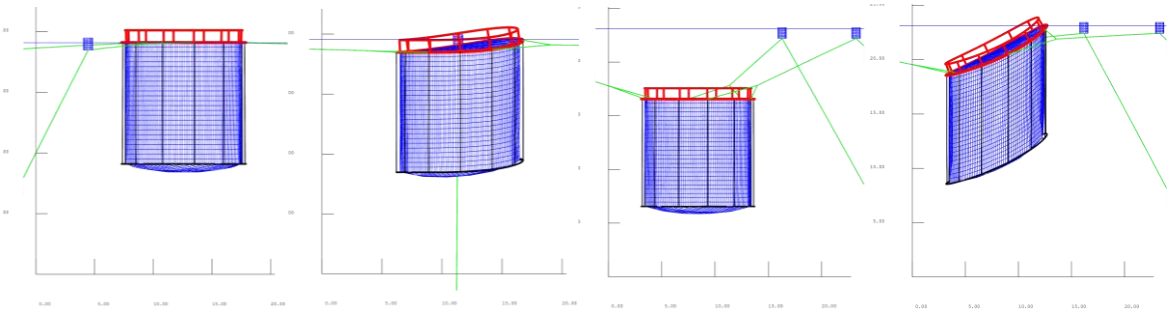

a b c d

**Figure 9**: (a) Cage at 0s, (b) 600s, (c) 1500s and (d) 2200s. At this last stage the volume inside the cage is minimal (figure 10).

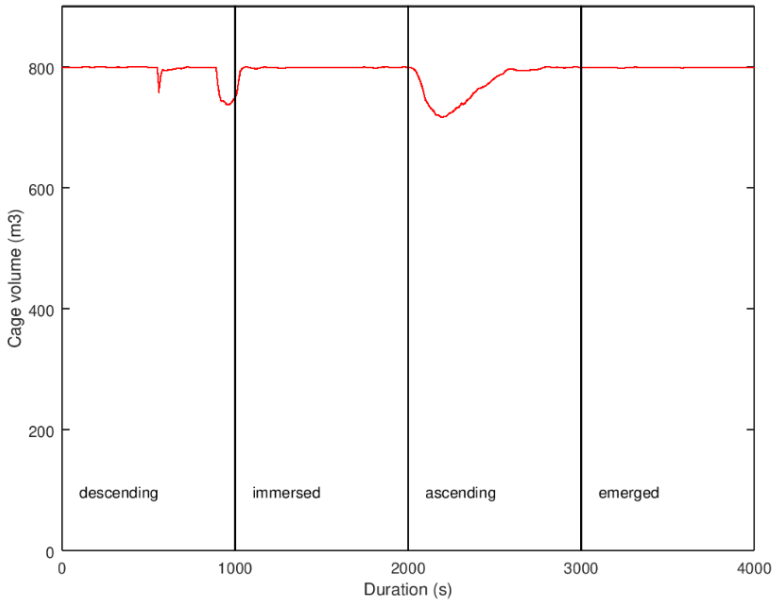

Figure 10: Variation of cage volume during the process of ballasting and unballasting. The mean value is 791 m³, the maximal is 800 m³ and the minimal is 717m³. The cage shape at the minimal value is visible on figure 9 (d).

Stress in the structure could increase during immersion: tension in the six bridles increases by 55% when the cage is immersed relative to the cage at the surface (left in figure11). However, maximal tension occurs when the structure is immersed, not during ballasting or unballasting.

As shown in figure 9 deformation of the floating part is significant. This deformation could lead to an increase in tension in the structure. On the right of figure 11, is the amplitude of tension in all bar elements of the handrail. There are 36 bar elements used for the handrail. The amplitude of tension is the absolute value of the tension. Thus, during ballasting and unballasting, noted "descending" and "ascending" on the right of figure 11, there is a large increase in tension amplitude: from 94N during the immersed and emerged phases up to 801N during the ascending phase. This value (801N) remains relatively small for this type of structure.

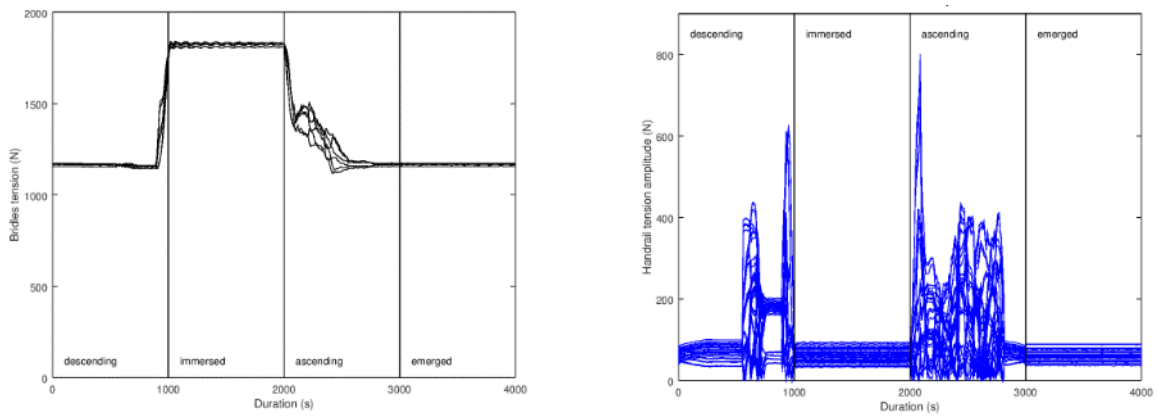


Figure 11: (Left) Tension in the six bridles. When the ballast is maximal (1500s), tension is considerably higher (+55%) than when there is no ballast (0s, and 4000s). (Right) Tension amplitude in the 36 handrail bar elements. Tension remains constant and low when the cage is immersed or emerged (<=94N). Tension increases considerably during the descending and ascending phases (<=801N).

## 4. DISCUSSION AND CONCLUSION

In the numerical modelling presented in this paper, a ballast tank is determined by a set of pipes (two pipes in figure 2 and figure 4; 27 pipes in figure 7). Each pipe of the ballast tank has a volume dedicated to the ballast. In the modelling, firstly, the ballast tank volume of each pipe is equally spread between the bar elements of the pipe. Secondly, this volume per bar is spread equally over each extremity of the bar element. Another modelling of the ballast tank is possible: instead of spreading firstly between bar elements and secondly between bar element extremities, it is possible to spread the volume of ballast tank directly between the nodes of bar elements. However, since this modelling provides good results, there is no need to change it.

Figure 5 shows a clear stair effect due to modelling parameters: Spreading the volume of ballast tank on cubes located at the extremities of bar elements, could lead to overlapping of cubes. This approximation is acceptable, as in figure 6 it is clear that the movement of a tube initially vertical is realistic.

It should be noted that there is no siphon effect applied in the present model: the water on the left of figure 4 could go on the right in the model although there is a high point which can determine a free surface of the ballast on the left which could be different as the free surface on the right. For this point, the present model is not realistic even if there is no risk of a siphon effect on our cage example, as shown in figure 9.

It should also be noted that the free surface remains horizontal in the present model. This approximation would be not valid in a real ballast tank, e.g. waves could occur. To make this approximation valid, the simulations shown here were carried out with a slow variation in ballast volume (2.412 m3 in 1000s for figure 9 and 0.083 m³ in 2000s in figure 6) to expect the free surface to remain horizontal.

The variation of ballast volume is a function of time as determined by the user. This point is highly questionable as we are sure that the variation of ballast is largely dependent on the conditions of this process. The water ballast may enter through pressure due to the depth of the cage. The flow rate of water could be affected by depth. The depth effect is not considered in this modelling, but could be introduced during future work.

So, we are able to assess the behaviour of fish cages using water ballast with our modelling. The shapes of the cage during the different phases (immersed, emerged, ballasting, unballasting) can be analysed. The tension in mooring lines or in the floating part, can also be analysed.

## REFERENCES

[1] M.Beveridge, 2004, Cage Cage aquaculture. 3rd ed. London: Blackwell Publishing. pp. 291–298.

[2] T.H.Kim, K.U.Yang, D.W.Fredriksson, The Submerging Characteristics of a Submersible Fish Cage System Operated by Compressed Air January 2010 Marine Technology Society Journal 44(1):57-68.

[3] D.Priour, 2013, A Finite Element Method for Netting: Application to fish cages and fishing gear. https://doi.org/10.1007/978-94-007-6844-4

[4] B.Morvan, D.Priour, Z.Guede, G.Bles, 2016, Finite element model for the assessment of the mesh resistance to opening of fishing nets, Ocean Engineering, Volume 123, 1 September 2016, Pages 303-313 https://doi.org/10.1016/j.oceaneng.2016.07.026

[5] Priour, D., 1999. Calculation of net shapes by the finite element method with triangular elements. Communications in Numerical Methods in Engineering, Volume 15, Issue 10, Pages 755-763.